Monodisperse Vesicles Stabilized by Grafted Polymers

R. Joannic,[1] L. Auvray,[1] and D. D. Lasic[2]
[1]*Laboratoire Léon Brillouin (CEA-CNRS), CEN Saclay, 91191 Gif-Sur-Yvette Cedex, France*
[2]*Liposomes Consultation, Newark, California 94560*
(Received 26 September 1996)

We have anchored an amphiphilic polymer on a fluid surfactant membrane. The polymer stabilizes the formation of vesicles over a wide composition and temperature range. The vesicles observed by light and neutron scattering are spontaneously spherical and monodisperse, and one can control their radius in the range 15–150 nm. They exhibit small shape fluctuations driven by their bending elasticity which we study quantitatively by dynamic light scattering. The polymer does not much influence the membrane rigidity in the range of the grafting density investigated but, nevertheless, locks the curvature of the vesicles. [S0031-9007(97)03033-0]

PACS numbers: 82.70.–y, 61.25.hq, 68.15.+e

One of the most successful ways of stabilizing colloidal particles against aggregation is to graft polymer chains at their surface [1]. In favorable cases, the grafted chains induce steric interactions between approaching surfaces, repulsive enough to prevent their sticking [2]. Recently, this idea has been applied to soft objects such as vesicles or liposomes, i.e., closed shells of self-assembled lipid bilayers [3], mimicking one of the possible functions of the outer polysaccharide layer of some biological cells. Polymers suitable for this purpose are, for example, the so-called polyethylene glycol (PEG)-lipids with a hydrophilic polyethylene glycol chain $[-(CH_2CH_2O)_n-]$ covalently attached to a double chain phospholipid molecule. The resulting "hairy" vesicles, designed for drug delivery, are efficiently protected against attacks by the immune system when injected in the blood [4].

Anchoring chains on vesicles may, however, lead to more complex phenomena than grafting polymers on solid undeformable surfaces. The chains may affect the equilibrium structure of the lipid aggregates, their shape, fluctuations, and elastic properties. These effects have been investigated theoretically [5–9] but not yet experimentally, in contrast to the more documented effects of the adsorption and confinement of homopolymers by surfactant membranes [10–12]. Numerous studies on "PEG-membranes" have focused mainly on the structure of the bilayers and their interactions [13], and not on the influence of grafted polymers on the formation and stability of vesicles. This influence is actually difficult to track in the case of PEG liposomes, because they are formed by a rather violent nonequilibrium process of extrusion and filtration, and also because their lipid bilayers are almost undeformable at a length scale of 100 nm, which is the size of these objects.

This is the reason why we have focused our interest on more flexible surfactant vesicles, formed spontaneously at thermal equilibrium, and studied their interactions with an amphiphilic polymer anchored on the surfactant bilayer. Thermodynamically stable vesicles can be obtained with several mixed systems of surfactants and co-surfactants [14–16]. For practical reasons (availability of the chemical species in the deuterated form), we have chosen to use as an initial model system a ternary mixture of sodium dodecyl sulfate [SDS, $CH_3(CH_2)_{11}OSO_3Na$], an anionic surfactant, octanol, and brine (2% NaCl in water by weight), which has recently been studied in detail [16]. The amphiphilic polymer we use is a commercially available polyoxyethylene-stearate, a single chain analog of the PEG-lipids, known as Myrj 59. The hydrophobic stearate group $[(CH_2)_{17}CH_3]$ is covalently linked to the end of a relatively short PEG chain containing 100 monomers (molecular weight, MW = 5000 D). We note that there is nothing special about this system since we have observed similar phenomena by using other surfactants, in particular, a cationic one and other amphiphilic co-polymers. In each case, the addition of co-polymers stabilizes a vesicle phase and leads to monodisperse vesicles of controlled size. We discuss here this new and general phenomenon according to the neutron and light scattering experiments that we have performed, including a quantitative observation of the shape fluctuations of the vesicles, which, until now, has only been studied on nonspontaneous giant phospholipid vesicles by light microscopy [3].

Myrj 59 is provided by Sigma, all other chemicals by Aldrich. To avoid the formation of nonequilibrium spherulites we dissolve the constituents in pure water where only micelles form. The final sample is then obtained by adding an equal volume of brine at a salinity of 4%. The mixture becomes progressively opalescent. At ambient temperature, the turbidity increases slowly and saturates after a time, varying between one week (for small polymer concentration) and 6 months (for higher polymer concentrations). One way of accelerating this process is to heat the samples. For example, sample b, shown in Fig. 1, heated at 55 °C for 7 min reaches the same state as the same sample held at 25 °C for 4 months. It thus appears that thermal aging is a way of monitoring the fusion and growth of the vesicles. If not specified, the samples are kept at 55 °C for 10 min and brought

 0031-9007/97/78(17)/3402(4)$10.00

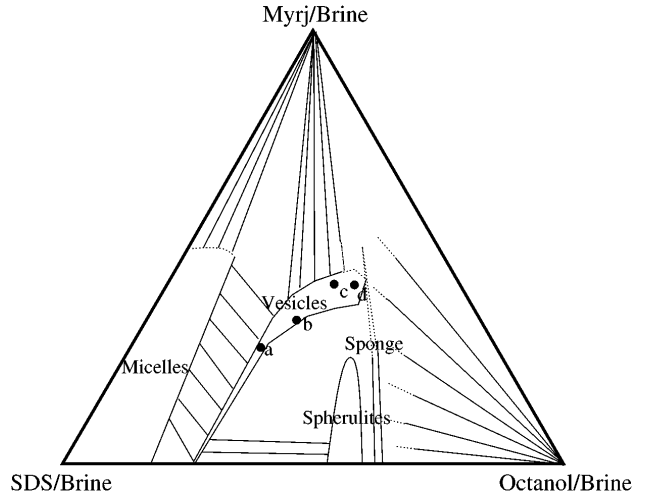

FIG. 1. Section of the phase diagram of the system SDS/octanol/Myrj 59 in brine ($T = 300$ K, NaCl = 2%) at fixed concentration of SDS (0.5%). At the center, the concentrations are (SDS 0.5% = 5 g/l, octanol 0.5% = 5 ml/l, Myrj 0.5% = 5 g/l). The compositions of samples a, b, c, and d are, respectively, a: (0.5, 0.28, 0.3), b: (0.5, 0.4, 0.5), c: (0.5, 0.7, 0.8), and d: (0.5, 0.9, 1). The dotted lines represent zones not investigated or difficult to evaluate, and continuous lines represent coexistence with other structures, micelles, or spherulites. Points a, b, c, and d are in the pure vesicle zone.

back to ambient temperature for at least one day before observation.

The stabilizing effect of the polymer on the vesicles is clearly observed on the phase diagram of the system in its water rich part (water volume fraction larger than 97%) (Fig. 1). Whereas the binary octanol/SDS vesicles only exist for a well-defined co-surfactant/surfactant ratio, and are destroyed by small changes of temperature and composition, ternary vesicles remain stable over a wide range of composition and temperature (between 10 °C and 60 °C).

As already observed [16] the vesicles without polymer have a very broad size distribution. Neutron scattering spectra exhibit the characteristic behavior of the intensity $I(q)$ scattered by a locally flat layer of finite thickness D [17]: $q^2I(q) = I_0[1 - \frac{(qD)^2}{12}]$ with $D = 1.8$ nm over the whole range of scattering vector q investigated. Static and dynamic light scattering spectra do not allow a size determination and only show that polydisperse objects with radii larger than 200 nm are present in the samples. The addition of polymer drastically changes this behavior. The simplest observations are made by light scattering or neutron scattering with nondeuterated constituants in heavy water. For sufficiently small vesicles of radius R smaller than 50 nm, for which we can record data in the relevant q range with a good resolution, the neutron scattering intensity oscillates strongly around a q^{-2} decay. The data of diluted samples are perfectly described by a model of noninteracting spherical shells with a narrow size distribution. The position and periodicity of the oscillations can be deduced from the form factor of a vesicle of radius R: $P(q) = 2\pi(\Delta n)^2 \frac{S}{V} D^2 q^{-2} \sin^2(qR)$, where Δn is the contrast, $\frac{S}{V}$ is the surface of the interface, and D is the thickness of the membrane. The oscillations are damped by the size and shape polydispersity. Neglecting for the moment the shape polydispersity and describing the size distribution of the vesicles by a normalized Schultz-Flory function [18], $F(R, \overline{R}, Z) = (\frac{Z+1}{\overline{R}})^{Z+1} \frac{R^Z}{\Gamma(Z+1)} e^{-(Z+1)R/\overline{R}}$, we deduce, by adjusting the parameters in the range $qD < 1$, the average radius of the vesicles $\overline{R}$ and the polydispersity index Z, related to the standard deviation of the radii distribution $\sigma_R^2 = \frac{1}{Z+1}$. The asymptotic behavior of the scattering intensity at a large scattering vector shows that we always get unilamellar vesicles and provides information on the membrane thickness and composition [17].

The most synthetic evidence for the existence of the peculiar "hairy vesicles" formed in this study is perhaps given by the neutron scattering observation of the samples under a contrast condition, where the surfactant and co-surfactant do not contribute to the scattering. This condition is achieved by making the samples with perdeuterated SDS and octanol in heavy water. Let us consider a sample close to the saturation line (point c in Fig. 1). Plotting $q^2I(q)$ against q as shown in Fig. 2, we recognize, at small q ($q < 0.4$ nm^{-1}), the oscillations of the form factor of a shell, which is here only revealed by the grafted polymer. We have to take into account in this case the rather large thickness L of the polymer bilayer, which is of the same order of magnitude as the vesicle average radius $\overline{R}$ and causes the fast decay of the quantity $q^2I(q)$ between 0.2 and 0.4 nm^{-1}. Assuming a constant density profile over the whole width of the polymer bilayer, we find, by adjustment, $\overline{R} = 22$ nm, $L = 15$ nm, and $Z = 13.5$. As it is known for grafted polymer layers [17], the behavior of the scattering intensity at a large scattering vector (here $q > 0.4$ nm^{-1}) cannot be interpreted in terms of interfacial concentration profile.

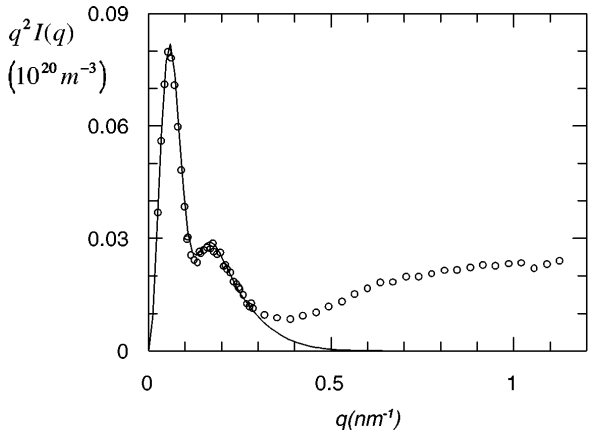

FIG. 2. Small angle neutron scattering spectrum of polymer in sample c. The continuous line is the fitted form factor of thick polydisperse spherical shells.

We observe in this range the monomer correlations in the inner structure of the polymer layer. The absolute value of the intensity is consistent in this case with the hypothesis of the total anchoring of the polymer on the surfactant membrane. We obtain an area per polymer chain $\Sigma_p = 14 \pm 2$ nm^2. The average distance between chains ($\Sigma_p^{1/2} = 3.7$ nm) is smaller than the thickness of a polymer monolayer (7.5 nm). The chains are thus slightly interpenetrated and interact at the surface. The value of 7.5 nm is of the same order of magnitude as the outer radius of a pure polymer micelle, 8 nm, which we have measured independently. More qualitatively, we conclude that the deformation of the chains and the resulting chemical potential are of the same order of magnitude in both situations, as it should be for saturated grafting at equilibrium.

The size of the vesicles depends strongly on their composition, aging time, and temperature, but the polydispersity remains small in the whole range of stability of the vesicle phase, with Z ranging between 13 and 20. The radius of the vesicles decreases almost linearly as both polymer and octanol are added to the membrane ($\overline{R}$ goes from 70 to 18 nm along line a-d of Fig. 1). For a given concentration the size increases with aging time and temperature. This last point is illustrated in Fig. 3, where we report the static light scattering intensity of six diluted samples of identical composition (sample b) heated at 55 °C for various times between 5 and 120 min. The mean radius increases from 40 to 114 nm. The data, plotted as $q^2 I(q)$ versus the reduced variable $q\overline{R}$, fall on the same master curve in the range $0.1 < q\overline{R} < 4$. This shows, in particular, that the membrane area and the vesicle polydispersity ($Z = 16$) are not changed by the thermal process. Note that heated for a longer time the vesicles keep on growing, but as their size increases at a constant surfactant concentration, their interactions increase and the system builds multilamellar vesicles of diameter $\simeq 0.5-1$ μm, observable by phase contrast microscopy and called spherulites in Fig. 1.

Since we were able to observe the inner structure of our largest vesicles, we attempted to detect their eventual internal modes of deformation by dynamic light scattering [19]. We have reported in Fig. 4 the normalized dynamical structure factors $\frac{I(q,t)}{I(q,0)}$ as a function of time for two scattering angles corresponding to $q\overline{R} = 0.8$ and $q\overline{R} = 3$. The curve recorded at small $q\overline{R}$ clearly represents the exponential relaxation due to translational Brownian motion. The second curve at $q\overline{R} = 3$ is not a pure exponential, and the relaxation at small times is faster than the translational relaxation.

Defining an effective diffusion coefficient D_{eff} by the initial slope of $\log \frac{I(q,t)}{I(q,0)}$ versus $q^2 t$, we obtain the results shown in Fig. 5, plotted in reduced units. The data define again a master curve with a pronounced maximum around $q\overline{R} = 3$. This is exactly the feature expected for small shape fluctuations of a spherical shell driven by bending elasticity which has until now only been observed in microemulsion systems by neutron spin echo spectroscopy [20]. By considering only size polydispersity and quadrupolar deformations, we obtain from [20]:

$$\overline{R} D_{\text{eff}}(q) = \frac{kT}{6\pi\eta} \times \left(h + \frac{9}{11} [4 j_2(x) - x j_3(x)]^2 \frac{A}{q^2 I(q,0)} \right),$$

where $x = q\overline{R}$, j_l is the spherical Bessel function of order l, η the viscosity of water, and $\frac{I(q,0)}{A}$ the static intensity normalized to $1/2q^2$ at large q. The h coefficient is defined as $h = \overline{R}/R_h$, R_h being the hydrodynamic radius. For a Schultz distribution, $h = \frac{(Z+1)}{(Z+4)}$.

As seen in Fig. 5 this expression reproduces satisfactorily the experimental results without adjustable parameter, Z and $I(q,0)$ being given by static experiments (Fig. 3).

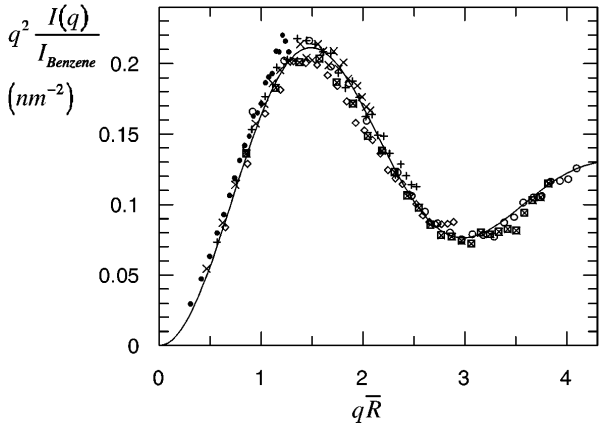

FIG. 3. Static light scattering data for vesicles (sample b diluted 5 times) of different radius in the representation $q^2 I(q)$ vs $q\overline{R}$: (•) $\overline{R} = 39$ nm, (×) 57 nm, (+) 70 nm, (◇) 80 nm, (□) 106 nm, and (∘) 114 nm. The continuous line is the fitted form factor of polydisperse thin spherical shells.

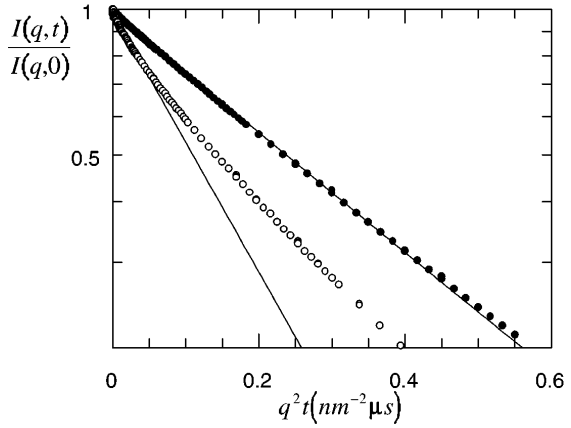

FIG. 4. Typical relaxation functions $I(q,t)/I(q,0)$ measured by light scattering in semilogarithmic representation. (•) $q\overline{R} = 0.8$ and (∘) $q\overline{R} = 3$. The straight lines have the initial slope of the relaxation functions.

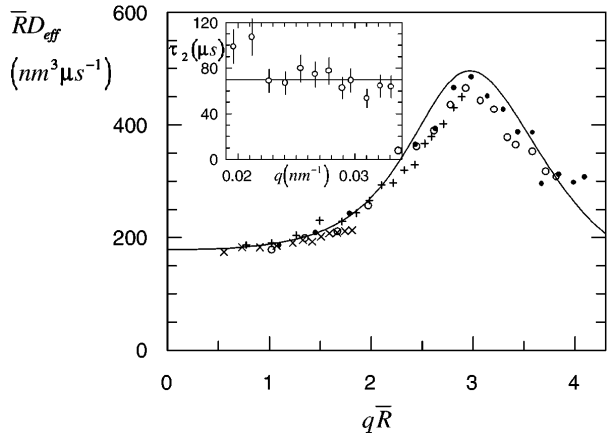

FIG. 5. Effective diffusion coefficient defined by the first cumulant of $I(q,t)/I(q,0)$, for vesicles of different radii $\overline{R}$: ($\times$) 57 nm, ($+$) 80 nm, ($\circ$) 106 nm, and ($\bullet$) 114 nm. The continuous line is the theoretical curve defined in the text. Inset: fast relaxation time as a function of q for the largest vesicles.

We conclude that the observed relaxation is indeed due to the translational motion and the ellipsoidal deformation both overdamped by the water viscosity. These two motions can be distinguished by fitting $\frac{I(q,t)}{I(q,0)}$ to a sum of two exponentials, in the vicinity of $q\overline{R} \simeq \pi$. The longer time which scales as $\frac{1}{Dq^2}$ is the translational diffusion. The shorter time (Fig. 5) is approximately constant $\tau_2 \simeq 70\ \mu$s. The amplitude of the corresponding quadrupolar mode, as defined in Ref. [19], is $\langle | u_2^2 | \rangle = 0.02$ for a vesicle of 114 nm.

The rigidity of the bilayer can be deduced if we assume that the membrane is without tension. We find $K = 2.1kT$, close to the estimated value for the bare vesicles [16,21], including the softening effect of octanol [22]. Thus, for the relatively small grafting densities obtained in this study, the polymer does not modify strongly the bilayer rigidity. This does not, however, imply that the bare and polymer coated vesicles are stable for the same reasons. We argue that, on the contrary, the mechanisms of stabilization are different in each case because the size distributions of the vesicles are very different. Several possibilities explain the spontaneous formation of vesicles: (a) a large translational entropy [23], (b) a negative Gaussian curvature energy [24], and (c) for mixed systems, the breaking of symmetry of composition of the outer and inner monolayer, which releases different local stresses imposed by the curvature. Causes (a) and (b) have been invoked in order to interpret the stability of the pure octanol-SDS vesicles [24] and explain satisfactorily their broad size distribution. Only cause (c) leads to a narrow size distribution [23]. Although our scattering experiments were not sensitive enough to detect a grafting asymmetry of the polymer, we think that it exists in our system. This symmetry breaking has been described in detail for polymer chains in the brush regime [5,6]; it may also be at work at the grafting densities studied here since even isolated chains tend to bend a membrane [7]. Finding evidence for this asymmetry will, of course, be the challenge for future experiments.

We thank M. Adam, D. Andelman, M. Geoghegan, D. Lairez, V. Ponsinet, and I. Talmon for useful discussions.

[1] D. Napper, *Polymeric Stabilisation of Colloidal Dispersions* (Academic Press, New York, 1983).
[2] P. Pincus, in *Lectures on Thermodynamics and Statistical Mechanics*, edited by A. Gonzales and C. Varea (World Scientific, Singapore, 1988), p. 74.
[3] D. Lasic, *Liposomes* (Elsevier, Amsterdam, 1993).
[4] *Stealth Liposomes*, edited by D. Lasic and F. Martin (CRC Press, Boca Raton, 1995).
[5] N. Dan and S. Safran, Europhys. Lett. **21**, 975 (1993).
[6] G. Porte and C. Ligoure, J. Chem. Phys. **102**, 4290 (1995).
[7] R. Lipowsky, Europhys. Lett. **30**, 197 (1995); C. Hiergeist and R. Lipowsky, J. Phys. II (France) (to be published).
[8] P.-G. de Gennes, J. Phys. Chem. **94**, 8407 (1990).
[9] K. Hristova and D. Needham, Macromolecules **28**, 991 (1995).
[10] H. Ringsdorf, J. Venzmer, and F. Winnik, Angew. Chem., Int. Ed. Engl. **30**, 315 (1991).
[11] C. Ligoure, G. Bouglet, and G. Porte, Phys. Rev. Lett. **71**, 3600 (1993).
[12] J. Lal and L. Auvray, J. Phys. II (France) **4**, 2119–2125 (1994).
[13] T. L. Kuhl, D. E. Leckband, D. D. Lasic, and J. N. Israelachvili, Biophys. J. **66**, 1479 (1996).
[14] E. Kaler, A. Murthy, B. Rodriguez, and J. Zasadzinski, Science **245**, 1371 (1989).
[15] W. Hargreaves and D. W. Deamer, Biochemistry **17**, 3759 (1978).
[16] P. Hervé, D. Roux, A.-M. Bellocq, F. Nallet, and T. Gulik-Krzywicki, J. Phys. II (France) **3**, 1255 (1993).
[17] P. Auroy, Y. Mir, and L. Auvray, Phys. Rev. Lett. **69**, 93 (1992).
[18] B. Zimm, J. Chem. Phys. **16**, 1093 (1948).
[19] S. T. Milner and S. A. Safran, Phys. Rev. A **36**, 4371 (1987).
[20] J. S. Huang, S. T. Milner, B. Farago, and D. Richter, Phys. Rev. Lett. **59**, 2600 (1987).
[21] E. Freyssingeas, Ph.D. thesis, Bordeaux, 1993 (unpublished).
[22] M. Bergström and J. C. Eriksson, Langmuir **12**, 624 (1996).
[23] S. A. Safran, P. A. Pincus, D. Andelman, and F. C. MacKintosh, Phys. Rev. A **43**, 1071 (1991).
[24] B. Simons and M. Cates, J. Phys. II (France) **2**, 1439 (1992).